ISBN: 978-3-95450-227-1 ISSN: 2673-5490 doi:10.18429/JACoW-IPAC2022-THPOST029

UPGRADE OF THE SLOW EXTRACTION SYSTEM OF THE HEIDELBERG ION-BEAM THERAPY CENTRE'S SYNCHROTRON

E. Feldmeier*, E. C. Cortés García, R. Cee, M. Galonska, Th. Haberer,
M. Hun, A. Peters, S. Scheloske and C. Schoemers, HIT, Heidelberg, Germany

Abstract

The Heidelberg Ion-Beam Therapy Centre HIT consists of a linear accelerator and a synchrotron to provide carbon ions, helium ions and protons for the clinical use as well as oxygen ions for experiments. The RF-KO slow extraction method is used to extract the particles from the synchrotron. To improve the spill quality of the extracted beam a new RF-signal was investigated which increases the R-value from 92.5% to 97.5% . The signal is a multiband RF signal broadened with a random BPSK at 3 frequency bands.

INTRODUCTION

The layout of the accelerator of the Heidelberg Ion Therapy Center HIT includes three ECR ion sources, an injector linac, a 6.5 Tm synchrotron and beam transport lines to deliver beam for the four target places: Two treatment rooms with a horizontally fixed beam-line, the heavy ion gantry and an experimental area.

The sources produces proton, helium and carbon beams for the medical treatment of localized tumors and oxygen beam for experiments.

The synchrotron accelerates the beam to an energy of up to 430 MeV/u for carbon ions, which corresponds to a penetration depth in water or human tissue of 30 cm.

RF Knock Out Slow Extraction

The beam is slowly extracted from the synchrotron by the radio frequency resonant knock out extraction method, the so called RF-KO extraction. A standard extraction time of 5 seconds with a constant intensity is used in this paper, in contrast to the raster point defined intensity modulation which is used in the routine operation described in [1].

SIGNAL GENERATION

The accelerator control system (ACS) provides the calculated set values from the data supply model in real time for the slow extraction. The Low-Level Radio Frequency (LLRF) signal is generated by a dedicated KO Direct Digital Synthesizer (KO DDS) and is delivered to the exciter by the broadband power amplifier (PA). The exciter generates the transverse electric field to excite the beam. The intensity feedback from [1] is delivered to the KO DDS to correct the pre-computed amplitude.

THE RF MULTIBAND SPECTRUM

The new RF KO spectrum consists of the sum of three single frequencies widened by a binary phase shift keying

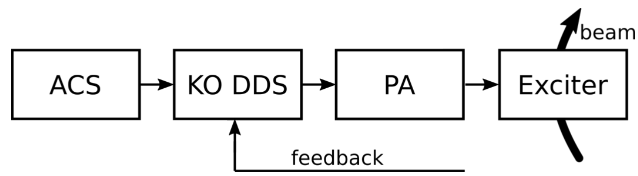

Figure 1: RF KO setup from the ACS, the Direct Digital Synthesizer (KO DDS), the power amplifier (PA) to the exciter, including the feedback for the intensity loop.

(BPSK) modulation. The two regions of interest found in the beam transfer function (BTF) signal [2, 3] near the betatron resonance were excited at the lower first harmonic and at the lower second harmonic. This is described in detail in WEPOTK022 on this conference [4].

The central frequencies are calculated by

$$\begin{aligned} f_1 &= (2 - q_1) \cdot f_{\mathrm{rev}} \\ f_2 &= (1 - q_0) \cdot f_{\mathrm{rev}} \\ f_3 &= (1 - q_1) \cdot f_{\mathrm{rev}} \end{aligned} \tag{1}$$

where q_0 is the fractional tune value of the nominal horizontal tune and q_1 represents the fractional tune value of the second peak found in the BTF signal at extraction conditions.

A signal of the form

$$U(t) = \cos\left(2\pi f_n t + \phi_{\mathrm{BPSK}}\right), \qquad n \in \{1, 2, 3\} \tag{2}$$

was generated for each of the three central frequencies f_n, where the pseudo-random binary phase shift keying (BPSK) ϕ_{BPSK} is given by

$$\phi_{\mathrm{BPSK}} = B \cdot \pi, \qquad B \in [0, 1]. \tag{3}$$

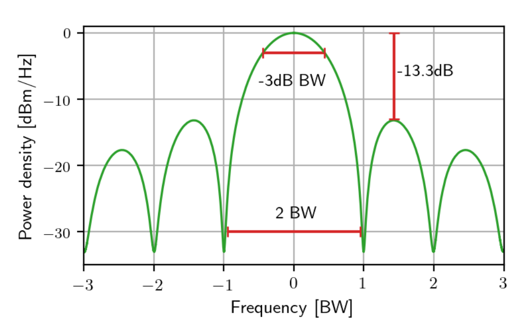

Figure 2: The symmetrical base band BPSK spectrum generated with a PRN has a -3 dB-bandwidth of BW = $f_{PRN,\mathrm{clock}}$, the zeros of the spectrum are at n·BW and the first side band is suppressed by -13.3 dB.

* eike.feldmeier@med.uni-heidelberg.de

ISBN: 978-3-95450-227-1 ISSN: 2673-5490 doi:10.18429/JACoW-IPAC2022-THPOST029

The pseudo-random noise (PRN) sequence B as a random binary sequence has a power density spectrum which is given by the auto-correlation function of $B(t)$, namely

$$B(\omega) \sim \left(\frac{\sin \omega}{\omega}\right)^2 . \tag{4}$$

A single band of the signal's spectrum is illustrated in Fig. 2. The -3 dB-point lies at $\pm f_{PRN,\mathrm{clock}}/2$. Therefore the -3 dB-bandwidth of the spectrum corresponds to BW $= f_{PRN,\mathrm{clock}}$. The immediate sidebands are suppressed by -13.3 dB, further sidebands are strongly suppressed, such that their contribution can be neglected.

To exemplify the aforementioned signal characteristics in Fig. 3 the KO spectrum for a carbon-ion beam E_{kin} = 124.25 MeV/u is shown. The three frequencies correspond to tune-values of q_0 and q_1 in the lower first and second harmonic. The bandwidth is set to 2 kHz for each peak, determined by experimental optimisation of the spill quality.

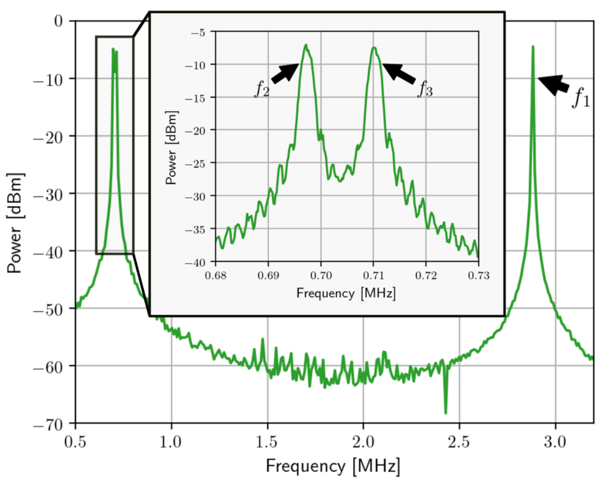

Figure 3: Exemplary excitation spectrum for the slow extraction of a carbon-ion beam with E_{kin} = 124.25 MeV/u. The three frequencies correspond to fractional tune values of $q_0 = 0.679$ and $q_1 = 0.673$, where both q-values are excited at the lower first harmonic and q_1 is also excited at the lower second harmonic.

The relation between voltage and power of the presented spectrum generation method is approximately $P \sim U^2$ and is optimal, since it exploits the full technical capacity of the power amplifier, if compared to other methods like the dual frequency modulation (FM) [5] or additive white gaussian noise (AWGN) [6, 7].

EXPERIMENTAL SETUP

To generate generic RF signals and spectra, an experimental setup was implemented (Fig. 4). It replaces the operational KO DDS with a Universal Software Radio Peripherial (USRP), which is provided with data by the open source software GNU Radio [8].

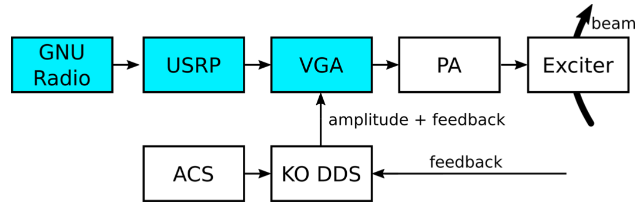

Figure 4: Block diagram of the experimental setup: The USRP generates the spectrum described above which is modulated by the variable gain amplifier (VGA) with the amplitude set value from the data supply model and the correction feedback loop provided by the ACS over the KO DDS. The LLRF signal is amplified by the PA and fed to the exciter.

Signal Generation With The USRP

GNU Radio includes ready to use building blocks to design the aforementioned RF signal, which is fed directly to the USRP. The generation of the three frequency bands is done independently and added afterwards. The model of each band consists of a random generator that feeds a 180°-phase shifter to the baseband generation and a mixer to get to the desired center frequency.

A variable gain amplifier (VGA) is used to modulate the amplitude of the RF signal with the given corrected amplitude by the feedback system.

KO-Exciter

The KO Exciter is a 50 Ω strip line exciter with a phase inverter between the two strip lines and a dummy load at the end of the second strip line. Its dimensions are a length of 70 cm and a width of 15 cm. The power amplifier has a maximum output power of $P = 400\,W$, thus the maximum available kick voltage $\hat{U}_{\mathrm{kick}}$ at the exciter is

$$\hat{U}_{\mathrm{kick}} = 2 \cdot \sqrt{P \cdot 50\,\Omega} \cdot \sqrt{2} = 400\,\mathrm{V}. \tag{5}$$

FINAL SETUP

Figure 5: The new KO DDS 2 consists of a FPGA based motherboard and a RF daughter board. It also includes the interlock system for spill pause and spill abort features.

A new direct digital synthesizer - the KO DDS 2 - was developed to generate the signal, first described in [2]. The

ISBN: 978-3-95450-227-1 ISSN: 2673-5490 doi:10.18429/JACoW-IPAC2022-THPOST029

new device is fully compatible with the ACS and fits in like the former DDS. It consists of an FPGA based motherboard and a daughter board which includes the RF modules. Due to semiconductor shortages the design was changed from a software based signal generation running on a modern FPGA to a more standard design with four independent DDS channels. Each path generates an amplitude modulated and in frequency broadened signal which is then combined in front of the final stage amplifier. The frequency, bandwidth and amplitude of each channel can be adjusted separately.

The specification of the KO DDS 2 is shown in Tab. 1.

Table 1: Specification of the KO DDS 2. Values in brackets are the maximum values, which are limited due to the specific usage.

Parameter	value
frequency range	0 - 5 (20) MHz
linearity	<1 dB
noise method	random BPSK
noise bandwidth	full frequency range
num. of ind. DDS	4
output power	-70 dBm to +10 dBm

SPILL IMPROVEMENTS

With the signal described above the spill was recorded with an ionisation chamber (IC) with a time resolution of 50 µs. A typical spill, with a fixed nominal intensity, is shown in Fig. 6 (blue) together with an improved spill extracted with the new excitation signal (orange). While the spill macrostructure is actively controlled by the feedback loop [1] the spill microstrucure was considerably improved. The fluctuations from the nominal value were diminished.

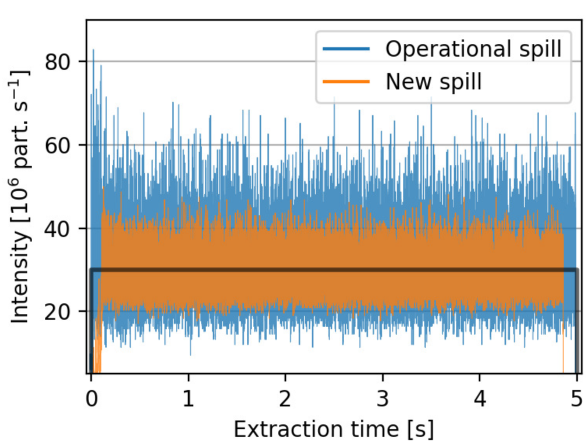

Figure 6: IC measurement of spills at 20 kHz with a carbon-ion beam C^{6+} with $E_{\mathrm{kin}} = 316.92$ MeV/u. Blue: Operational spill recorded with the nominal scheme for extraction. Orange: Spill recorded with the described signal.

Spill Duty Factor

The spill duty factor is defined as [9, 10]

$$R = \left. \frac{\langle x \rangle^2}{\langle x^2 \rangle} \right|_T , \tag{6}$$

where x is typically the read-out of a ionisation chamber's current or a particle count per unit time. The spill duty factor is a measurand of the spill quality since the higher the fluctuations are, the higher the denominator becomes, which translate in 'low' spill quality. The averaging time T of the spill duty factor R is varied depending on the time-scale of interest.

Since the irradiation of a raster point is in the range of a few milliseconds, the spill duty factor R is presented for a nominal 5 second spill within a 1 ms windows.

Spills were recorded over representative extraction energies for the proton and carbon-ion beams.

The described signal delivered a considerable improvement of the spill duty factor over the entire extraction energy range. While the spill duty factor of the carbon-ion beam was already high, with the new excitation RF signal it is now kept always over the 90% level. The improvement is more significant for the proton beam, since for some energies the duty factor could drop as low as 60% and is now kept over the 90% level as well. For the full results, please see [3].

CONCLUSION

The micro spill structure was improved tremendously. The above described spill duty-factor was increased for some energies from 60% to over 90%.

For clinical use, this is a great improvement. Since one limitation in the speed of beam application in treatment mode is an upper limit of the intensity one cannot exceed. The limit value is intended to ensure that the measurement time per raster point is sufficient for proper irradiation. A violation of this limit leads to an abort of the irradiation and needs some time for manual reset. High fluctuations with high peaks but short in time, which are represented by a low spill duty factor, can trip such an interlock. To prevent these interlocks, a safety margin between the intensity set value and the intensity limit is used to lower the set value to about 25%.

With the shown improvement of the spill duty factor, this safety margin can be reduced, which increases the set value and instantaneously reduces the irradiation time of the treatment. A doubling of the set value to 50% of the limit is conceivable. The maximal achievable benefit will be examined next.

The shown improvements were achieved by just changing the RF signal for the KO excitation process. The noise generation for the generation of the RF bandwidth was selected in such a way that the given amplifier power is optimally utilized. However, other methods of noise generation can also be used.

ISBN: 978-3-95450-227-1 ISSN: 2673-5490 doi:10.18429/JACoW-IPAC2022-THPOST029

REFERENCES

[1] C. Schoemers, E. Feldmeier, J. Naumann, R. Panse, A. Peters, and T. Haberer, "The intensity feedback system at Heidelberg Ion-Beam Therapy Centre", *Nucl. Instrum. Methods Phys. Res., Sect. A*, vol. 795, pp. 92–99, 2015.

[2] E. C. Cortés García, "Investigation of RF-signals for the slow extraction at HIT's medical synchrotron", M.Sc. thesis, TU Darmstadt, Germany, http://tuprints.ulb.tu-darmstadt.de/20811

[3] E. C. Cortés García, E. Feldmeier, M. Galonska, C. Schömers, M. Hun, S. Brons, R. Cee, S. Scheloske, A. Peters, and Th. Haberer, "Optimization of the spill quality for the hadron therapy at the Heidelberg Ion-Beam Therapy Centre",*Nucl. Instrum. Methods Phys. Res., Sect. A*, to be published, 2022.

[4] E. C. Cortés García, E. Feldmeier, and Th. Haberer (HIT, Heidelberg, Germany), "Horizontal beam response at extraction conditions at the Heidelberg Ion-Beam Therapy Centre", presented at the IPAC'22, Bangkok, Thailand, Jun. 2022, paper WEPOTK022, this conference.

[5] K. Noda, M. Kanazawa, A. Itano, E. Takada, M. Torikoshi, N. Araki, J. Yoshizawa, K. Sato, S. Yamada, H. Ogawa, H. Itoh, A. Noda, M. Tomizawa, and M. Yoshizawa, "Slow beam extraction by a transverse RF field with AM and FM", *Nucl. Instrum. Methods Phys. Res., Sect. A*, vol. 374, no. 2, pp. 269–277, 1996.

[6] T. Nakanishi, "Dependence of a frequency bandwidth on a spill structure in the RF-knockout extraction", *Nucl. Instrum. Methods Phys. Res., Sect. A*, vol. 621, no. 1, pp. 62–67, 2010.

[7] T. Yamaguchi, Y. Okugawa, T. Shiokawa, T. Kurita, and T. Nakanishi, "Slow beam extraction from a synchrotron using a radio frequency knockout system with a broadband colored noise signal", *Nucl. Instrum. Methods Phys. Res., Sect. B*, vol. 462, pp. 177–181, 2020.

[8] GNU Radio, https://www.gnuradio.org/.

[9] P. Forck, "Measurement technique for micro and millisecond spill structures", presented at the *1st Slow Extraction Workshop*, Darmstadt, Germany, Jun. 2016, https://indico.gsi.de/event/4496/sessions/3264/#20160601

[10] R. Singh, P. Forck, and S. Sorge, "Reducing fluctuations in slow-extraction beam spill using transit-time-dependent tune modulation", *Phys. Rev. Applied*, vol. 13, Iss. 4, 044076, 2020.